Abdullah Sinan Ahmed[1], Hassan Falah Hassan[2], Mutaz Kadhim Medhlom[2]

BEHAVIOUR OF TWO-WAY FIBROUS HIGH STRENGTH CONCRETE SLABS REINFORCED WITH GFRP BARS UNDER UNIFORMLY DISTRIBUTED LOADS

PONAŠANJE RAVNOMERNO OPTEREĆENIH PLOČA SA PRENOSOM OPTEREĆENJA U DVA PRAVCA, KOJE SU IZRAĐENE OD VLAKNASTO OJAČANOG BETONA VISOKE ČVRSTOĆE ARMIRANOG GFRP ŠTAPOVIMA

Originalni naučni rad / Original scientific paper
UDK /UDC:

Rad primljen / Paper received: 20.03.2020

Adresa autora / Author's address:
[1)] Al-Mansour University College, Civil Engineering Department, Baghdad, Iraq
[2)] Al-Mustansiriyah University, Faculty of Engineering, Civil Engineering Department, Baghdad, Iraq email: hassanfala@gmail.com, hassanfalah@uomustansiriyah.edu.iq

Keywords
- GFRP bars
- high-strength concrete
- fiber concrete
- two-way slab
- uniformly distributed loads
- ANSYS®

Ključne reči
- štap od polimera ojačan staklenim vlaknima (GFRP)
- beton visoke čvrstoće
- vlaknasti beton
- ploča sa prenosom opterećenja u dva pravca
- uniformna raspodela opterećenja
- ANSYS®

Abstract

The replacement of conventional steel reinforcement with glass-fiber reinforced polymer (GFRP) bars is investigated to overcome the problem of corrosion of steel reinforcement which causes most of the failures in concrete structures, especially in harsh environments. However, the lower modulus of elasticity of GFRP bars and their non-yielding characteristics results in large deflection and wide cracks in GFRP reinforced concrete members. Hence, there is an essential need for a suitable design philosophy and for methods that can provide a reliable estimate of such behaviour.

The behaviour is evaluated of simply supported concrete slabs reinforced with GFRP bars and subjected to uniformly distributed loads. The slabs had sizes 800×450×50 or 70 mm with different reinforcement and steel fiber ratios. This research investigates the flexural and shears limit states of slabs, including pre-cracking behaviour, cracking pattern, ultimate crack width, deflection, failure mode, and ultimate loads. The information presented is valuable for the development of design guidelines for FRP-reinforced concrete structures. Three dimensional finite element analyses by using ANSYS® software is performed as verification of all experimental slabs.

Izvod

Istražena je zamena armaturnih štapova, konvencionalnih čelično ojačanih, sa štapovima od polimera ojačanih staklenim vlaknima (GFRP), kako bi se rešio problem korozije čelične armature, koja često izaziva lom u betonskim konstrukcijama, posebno u teškim uslovima sredine. Međutim, manji modul elastičnosti kod GFRP štapova kao i njihove karakteristike bez pojave tečenja, rezultuje u pojavi velikog ugiba i u širim prslinama unutar GFRP ojačanih betonskih elemenata. Stoga, javlja se potreba za odgovarajućom filozofijom u projektovanju i u postupcima, kojima se može postići pouzdanija procena ponašanja konstrukcije.

Izvedena je procena ponašanja prosto oslonjenih betonskih ploča, ojačanih GFRP štapovima, podvrgnutih ravnomernom opterećenju. Ploče su dimenzija 800×450×50 ili 70 mm, sa različitim udelom ojačanja i čeličnih vlakana. U radu se istražuje granično stanje pri savijanju i smicanju ploče, kao i ponašanje sa početnom prslinom, razvojem prsline, graničnom širinom prsline, ugibom, tipom loma, i pri graničnim opterećenjima. Predstavljeni rezultati su od značaja za razvoj preporuka za projektovanje polimer-vlaknasto ojačanih betonskih konstrukcija. Izvedena je analiza trodimenzionalnim konačnim elementima primenom softvera ANSYS®, radi provere svih eksperimentalnih ploča.

INTRODUCTION

The use of non-metallic reinforcement (GFRP) as an alternative to steel reinforcement in concrete structures, particularly in harsh and aggressive environments, is gaining acceptance mainly due to its high corrosion resistance, and its high mechanical performance, /1/. In comparison to steel, the distinctive properties of GFRP bars are high strength, relatively low modulus of elasticity, and elastic response to failure. Due to the lower modulus of elasticity of the GFRP bars compared to that of steel, for the same reinforcement ratio, GFRP-reinforced concrete members will exhibit larger deflections and crack widths, also the failure mechanism is relatively brittle, even in bending. This gives rise to major concerns by structural designers who are more familiar with the under-reinforced design philosophy developed for steel reinforced concrete members, which ensures a ductile failure before collapse. To facilitate the rapid adoption of GFRP in concrete construction, most researchers working in this field have attempted to provide

simple design equations, many design provisions and guidelines are available for the design of concrete beams or slabs reinforced with GFRP bars: these include the Japan Society of Civil Engineers Design Provisions (JSCE 1997) /2/, the Canadian Design Provisions (CAN/CSA-S806-02) /3/, the American Concrete Institute Guidelines (ACI 440.1R-06) /4/, and the American Association of State Highway and Transportation Officials Load Resistance Factor Design (LRFD), Bridge Design Guide Specifications for GFRP Reinforced Concrete Decks (AASHTO 2009) /5/. In the last decade, considerable efforts have been made to apply FRP composites in the construction industry, and recently, structural applications of FRP composites started to appear in civil infrastructure systems. FRP composite materials have been used as internal and external reinforcement in the field of civil engineering constructions. It has been used as internal reinforcement for beams, slabs, and pavements /6, 7/, and also as external reinforcement for rehabilitation and strengthening different structures, /8, 9/.

Although the use of steel fiber reinforced concrete (SFRC) has been increasing over the past two decades, the anticipated implementation of SFRC may have been hindered by a lack of guidelines and knowledge concerning the influence on structural behaviour, e.g. plastic redistribution. Extensive research has proved that steel fibers provide significant post-crack ductility to the otherwise brittle concrete. This effect has been quantified in numerous studies /10-12/ and standards have been developed for assessing characteristic material parameters, e.g. fracture energy /13, 14/. A common application of SFRC is in industrial flooring, i.e. slabs on ground /15, 16/. More recently, SFRC has also been used as the only type of reinforcement in elevated slabs, /17/, or in combination with conventional reinforcement, /18/. Documented benefits of SFRC include both the bending /15, 19/ and shear capacity /20/ of slabs. In the design of two-way reinforced concrete slabs, e.g. using the strip or yield line design method, the possibility of redistributing the load between different load-carrying directions is commonly used.

Research significance

The flexural behaviour of two-way fibrous high strength concrete (FHSC) slabs reinforced with GFRP bars under uniformly distributed loads has yet to be fully investigated. The research describes the various limit states behaviour including modes of failure due to variation of the slab thickness, steel fiber content and the reinforcement ratio. The information gathered throughout this investigation is valuable for future development of design guidelines for two-way FHSC concrete slabs. It also assesses the accuracy of current equations predicting the flexural capacity of GFRP reinforced concrete members.

EXPERIMENTAL PROGRAM

The experimental work of this study consists of casting and testing twelve simply supported reinforced concrete slabs under uniformly distributed loads. Details of all experimental work stages are presented as followed.

Materials

- Cement

Ordinary Portland cement (type I) manufactured by the united cement company (UCC) in Iraq is used throughout the experimental work of this study.

- Aggregate

Natural sand is used as fine aggregate and crushed river gravel with maximum particle size of 10 mm for all mixes.

- High range water reducing admixture

The high range water reducing admixture used in this study is a third generation polycarboxylates co-polymer liquid, known commercially as Viscocrete-PC20. It is imported from the Sika Company in Turkey.

- Steel fibers

Hooked short steel fibers are used throughout the experimental program; the properties of the used steel fibers are presented in Table 1.

Table 1. Properties of the used steel fibers*.

Property	Specifications
Relative density	7860 kg/m^3
Ultimate strength	2000 MPa
Modulus of elasticity	200×10^3 MPa
Strain at proportion limit	5650×10^{-6}
Poisson's ratio	0.28
Average length	30 mm
Nominal diameter	0.375 mm
Aspect ratio (L_f/D_f)	80

*According to the certificate of conformity

- GFRP reinforcement

Deformed GFRP bars of nominal diameter 7 mm are used as slab reinforcement. They are imported from Armastek Company in Iran. Table 2 shows the properties of the GFRP bars used in this study.

Table 2. Properties of GFRP bars *.

Weight (kg/m)	Elongation (%)	Ultimate strength (MPa)	Tensile modulus of elasticity (MPa)
0.07	2.2	1200	55000

*According to the certificate of conformity.

Details of the test slabs

Twelve slabs of dimensions 800×450×50 or 70 mm are cast and tested in flexure under uniformly distributed loads in this study. Eight of these slabs are made with HSC and four with FHSC. During loading the slabs are simply supported at their ends on steel beams which formed part of a rigid steel frame.

Three variables are investigated in this research to show their effects on the flexural strength of the FHSC two-way slabs. These variables are:

1. percentage of steel fibers,
2. flexural steel reinforcement ratio,
3. thickness of the slab.

Table 3 illustrates the details of all the test slabs.

Slabs designations are as following:

1st symbol (H) from high.
2nd symbol (S) from strength.
3rd symbol (S) from slab.

4th symbol (1, 2, 3 and 4) from ρ_1, ρ_2, ρ_3 and ρ_4.
5th symbol (0, 0.5 and 1) from steel fiber content, V_f = 0, 0.5 or 1%.
6th symbol (5 and 7) from slab thickness, 50 or 70 mm.

Table 3. Details of all the test slabs in the present research.

Slab designation	Steel reinforcement ratio (ρ)	Steel fibers % by volume	Slab thickness (mm)
HSS1-0-5	0.0048	0	50
HSS1-0-7	0.0032	0	70
HSS2-0-5	0.0074	0	50
HSS2-0-7	0.0049	0	70
HSS3-0-5	0.0096	0	50
HSS3-0-7	0.0064	0	70
HSS4-0-5	0.012	0	50
HSS4-0-7	0.008	0	70
HSS1-0.5-5	0.0048	0.5	50
HSS1-0.5-7	0.0032	0.5	70
HSS1-1-5	0.0074	1	50
HSS1-1-7	0.0049	1	70

Mix proportions and concrete mechanical properties

Table 4 gives mix proportions and mechanical properties of FHSC mixes used in different slabs. Based on several trial mixes, three FHSC mixes that differ from each other only in volumetric steel fiber ratio (V_f) are adopted in this study.

Table 4. Mix proportions of CC and FHSC.

Concrete Type	HSSCC		
Cement (C) (kg/m^3)	550		
Sand (S) (kg/m^3)	460		
Gravel (G) (kg/m^3)	1085		
Superplasticizer (SP) (kg/m^3)	14		
Water (W) (kg/m^3)	165		
W/C	0. 3		
Steel fibers (kg/m^3)	0	39	78.5
V_f (%)	0	0.5	1
Cylinder compressive strength (MPa)	72	78	81
Modulus of rupture (MPa)	5.1	5.9	6.75
Tensile splitting strength (MPa)	7.6	8.9	9.7
Modulus of elasticity (MPa)	39982	41530	42600

System of loading and testing procedure

Uniformly distributed load is the most common load encountered in practice. In the laboratory such load can be produced by using a large number of point loads applied through hydraulic jacks, for example Wood /21/ used 16 point loads distributed uniformly over the entire surface of the slab to represent uniform loading, while Johansen /22/ used 24 point loads to obtain uniformly distributed loading (UDL). Alternatively, hydrostatic, or pneumatic pressure can be applied on a test slab as used by Hayes /23/, while Sawczuk and Winnicki /24/ and Park /25/ achieved UDL by applying water pressure to the bottom face of the slab. The uniform load can somehow be produced using sand as adopted by Al-Shadidi /26/ and Hassan /27/. In this research, the uniform load was furnished as follows:

a) using one layer of 50 mm diameter steel ball distributed uniformly over the entire surface of the slab held in position by using a steel box placed on the slab directly over the supports (as shown in Fig. 1),
b) more loading is applied using small sacks of sand distributed uniformly over the layer of steel balls,
c) in cases of restrained slabs, additional load is added on the slab using fragments of steel distributed over the sacks of sand.

It is to be noted that the steel box placed on the slab periphery is coated with a sheet of nylon to prevent any possible friction between the ingredients of the applied load and the inner surface of the steel box. This system of loading had caused the slab to fail in form of patterns which were satisfactory with the patterns adopted theoretically, as is observed in the next articles.

A dial gauge of 50 mm maximum reading is used to measure the vertical deflection of the test slabs at centre for every increment of the applied loading. The procedure of loading and deflection measurement continued until excessive values of deflections are recorded indicating that the slab is on the verge of failure.

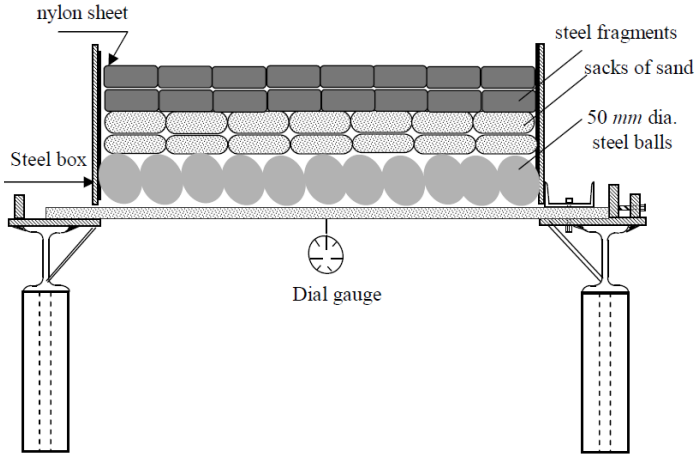

Figure 1. The loading system used to represent the uniform load.

EXPERIMENTAL RESULTS AND DISCUSSION

Ultimate strength and first crack loading

Table 5 summarizes the results of first cracking load (P_{cr}), ultimate load (P_u) and mode of failure for all tested slabs together with their deflection.

Table 5. Ultimate and first cracking load of the tested slabs.

Slab design.	Concrete compr. strength (N/mm^2)	P_{cr} (kN)	P_u (kN)	P_{cr}/P_u	Deflec. at P_u (mm)	Deflec. at P_{cr} (mm)	Failure modes*
HSS1-0-5	72	20	82.5	0.24	1.25	0.155	G.R.
HSS1-0-7	72	24	93.5	0.256	2.8	0.32	G.R.
HSS2-0-5	72	22.5	90	0.25	2.6	0.26	G.R.
HSS2-0-7	72	29.5	107.5	0.274	1.6	0.232	G.R.
HSS3-0-5	72	35	112.5	0.31	2.2	0.3	C.C.
HSS3-0-7	72	42	135	0.31	2.45	0.27	C.C.
HSS4-0-5	72	43.2	120	0.36	2.2	0.245	C.C.
HSS4-0-7	72	55.5	160	0.347	3.65	0.648	C.C.
HSS1-0.5-5	78	39.5	98.5	0.4	2.6	0.385	C.C.
HSS1-0.5-7	78	43	102.5	0.42	2.1	0.3	C.C.
HSS1-1-5	81	72	147.5	0.488	2.58	0.7	C.C.
HSS1-1-7	81	76	152.5	0.498	2.9	0.8	C.C.

* C.C: concrete crushing, G.R: GFRP bar rupture.

Effect of GFRP reinforcement ratio

Generally, the ultimate flexural capacity increases with the addition of GFRP reinforcement.

The percentages increase of the ultimate failure load in slabs of 50 mm thickness are increased to 13.33, 36.36 and 45.45 % when the GFRP reinforcement ratio increases from 0.0048 to 0.0074, 0.0096 and 0.012, respectively.

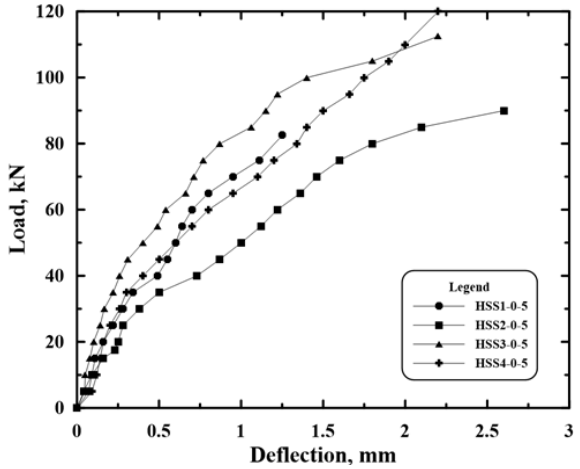

Figure 2. Effect of GFRP reinforced ratio on load-deflection behaviour of 50 mm thick slab.

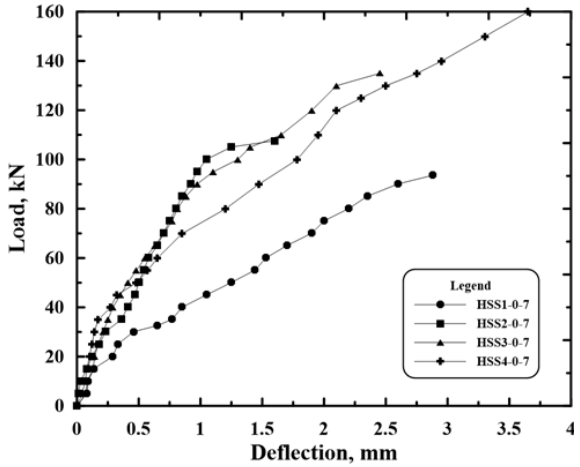

Figure 3. Effect of GFRP reinforced ratio on load-deflection behaviour of 70 mm thick slab.

Table 6. Effect of GFRP reinforcement ratio on ultimate load of the tested slabs.

Slab design.	Slab thickness (mm)	P_u (kN)	Increase ratio (%)
HSS1-0-5	50	82.5	0
HSS2-0-5		90	13.33
HSS3-0-5		112.5	36.36
HSS4-0-5		120	45.45
HSS1-0-7	70	93.5	0
HSS2-0-7		107.5	15
HSS3-0-7		135	44.4
HSS4-0-7		160	71.1

On the other hand, the percentages of increased ultimate failure load in slabs of 70 mm thickness by 15, 44.4 and 71.1 % when the GFRP reinforcement ratio increase from 0.0032 to 0.0049, 0.0064 and 0.008, respectively. Table 6 and Figs. 2 and 3 show the effect of flexural GFRP reinforcement ratio on the ultimate failure load.

From the results in Table 6, one can see that the percentage increases of the ultimate failure load for slabs of 70 mm thickness are always higher than percentages in the slabs of 50 mm thickness.

Effect of volume fraction of steel fibers (V_f)

Table 7 and Figs. 4 and 5 show the effect of the addition of steel fibers on the ultimate and first cracking load of the tested slabs. With the addition of steel fibers, both the first cracking and ultimate failure loads increase. However, the increase in the ultimate load seems more regular and significant than that in the cracking load. This behaviour may be attributed to the enhanced stiffness of the slab and improved mechanical properties of concrete, such as the modulus of elasticity, tensile strength, and compressive strength, when the amount of steel fibers is increased.

Table 7. Effect of steel fiber content on ultimate- and first cracking load of the tested slabs.

Slab design.	Slab thick. (mm)	Steel fiber (%)	P_{cr} (kN)	P_u (kN)	P_{cr}/P_u	P_u increase ratio (%)	P_{cr}/P_u increase ratio (%)
HSS1-0-5	50	0	20	82.5	0.24	0	0
HSS1-0.5-5		0.5	39.5	98.5	0.4	19.4	60
HSS1-1-5		1	72	147.5	0.488	78.78	103
HSS1-0-7	70	0	24	93.5	0.256	0	0
HSS1-0.5-7		0.5	43	102.5	0.42	9.6	64
HSS1-1-7		1	76	152.5	0.498	63.1	91

Results indicate that flexural strength of slabs against cracking can be enhanced upon the addition of steel fibers. The increase in cracking load is higher for higher steel fiber contents. Results also show that cracking load is more affected than ultimate load by using different volumes of fibers.

The steel fibers result in a more ductile type of failure. Slabs with fibers have exhibited considerably less damage at failure than slabs without fibers. Besides, they also exhibited more uniform cracking and smaller observed crack width at all stages of loading. Figure 8 shows the effect of steel fibers on cracks pattern of tested slabs, it is obvious that the crack width is smaller when using fibers. It is also noticed that ductile behaviour and slower crack propagation occurs during the test.

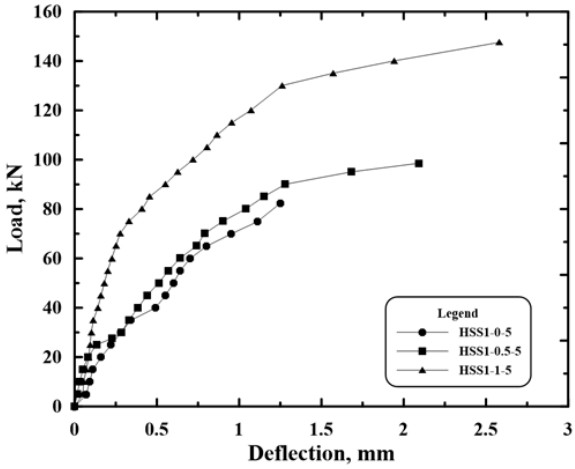

Figure 4. Effect of steel fiber content on load-deflection behaviour of 50 mm thick slab.

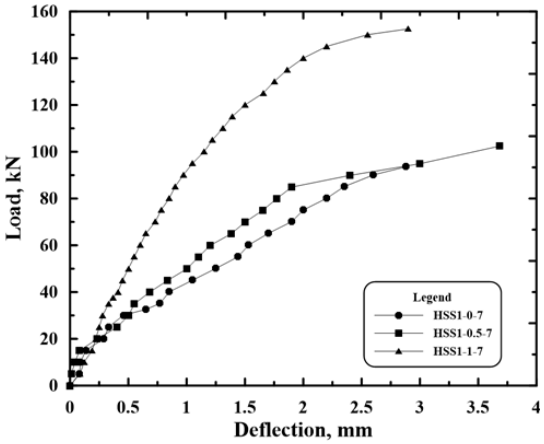

Figure 5. Effect of steel fiber content on load-deflection behaviour of 70 mm thick slab.

Effect of slab thickness

Generally, the ultimate flexural capacity increases with the increase of slab thickness.

For non-fibrous concrete, an increase in slab thickness from 50 to 70 mm increases the ultimate failure load by 13.33, 19.44, 11.11 and 33.33 %, for slabs with 0.0048 (0.0032), 0.0074 (0.0049), 0.0096 (0.0064) and 0.012 (0.008) flexural steel reinforcement ratio, respectively, where numbers in brackets are for 70 mm slabs.

Percentage increase of the ultimate failure load in fibrous concrete slabs are 4.1 and 3.4 % for slabs with steel fiber content 0.5 and 1 %, respectively. Table 8 and Figs. 6 and 7 show the effect of slab thickness on the ultimate failure load.

Table 8. Ultimate and first cracking load of the tested slabs.

Slab design.	Slab thick. (mm)	Steel reinf. ratio (ρ)	P_u (kN)	Increase of ratio (%)
HSS1-0-5	50	0.0048 (0.0032)*	82.5	13.33
HSS1-0-7	70		93.5	
HSS2-0-5	50	0.0074 (0.0049)*	90	19.44
HSS2-0-7	70		107.5	
HSS3-0-5	50	0.0096 (0.0064)*	112.5	11.11
HSS3-0-7	70		135	
HSS4-0-5	50	0.012 (0.008)*	120	33.33
HSS4-0-7	70		160	
HSS1-0.5-5	50	0.0048 (0.0032)*	98.5	4.1
HSS1-0.5-7	70		102.5	
HSS1-1-5	50	0.0074 (0.0049)*	147.5	3.4
HSS1-1-7	70		152.5	

* Reinf. ratio for 70 mm slabs is the same (ρ) for 50 mm slabs.

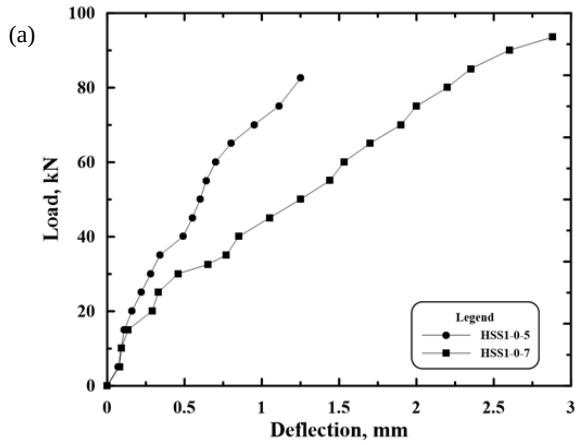

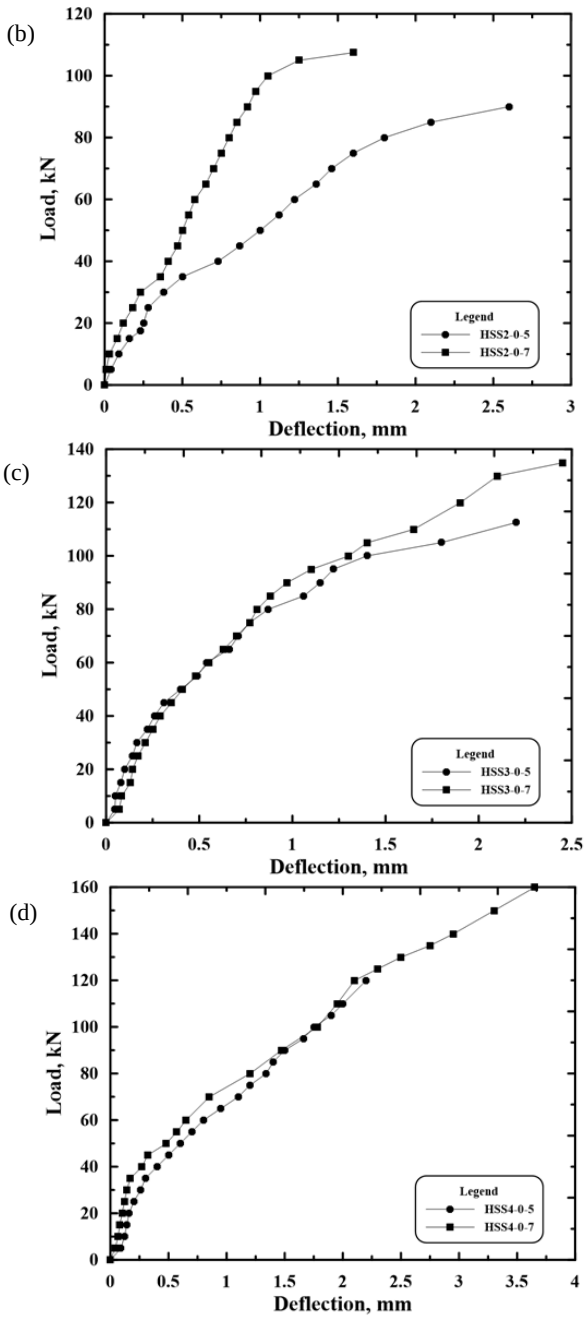

Figure 6. Effect of slab thickness on load-deflection of non-fibrous concrete slab at ρ values: a) 0.0032, b) 0.0049, c) 0.0064, d) 0.008.

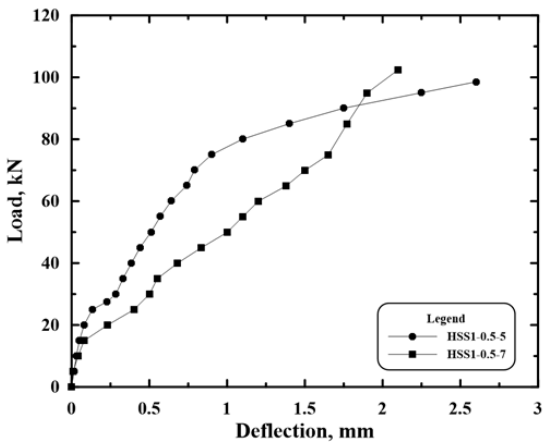

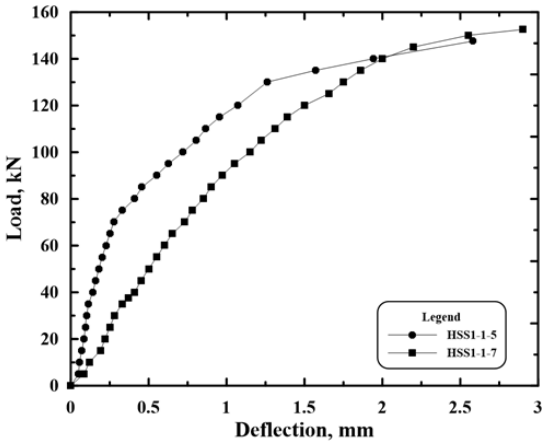

Figure 7. Effect of steel fiber content on load-deflection behaviour of fibrous concrete slab.

Load-deflection relationships

Figures 2 to 7 show the mid-span deflection versus applied loads for the tested slabs and the effect of variable parameters considered in this study (reinforcement ratio, slab thickness, and steel fiber content). For all tested slabs, the load-deflection relationship is a nearly bilinear response up to failure. The specimens had approximately a similar stiffness up to the initiation of the first crack, followed by a reduction in stiffness for all slabs, but with different tendencies. After the cracking stage, the stiffness's of tested slabs were dependent on the axial stiffness of the reinforcing bars. Figures 2 and 3 show the effect of the GFRP reinforcement ratio for non-fibrous concrete slab thickness of 50 and 70 mm, respectively, on the deflection behaviour.

Adding steel fibers to concrete is known to enhance the concrete microcracking and consequently the concrete tensile strength. Figures 4 and 5 represent the effect of the amount of steel fibers added to the concrete mix for slabs with 50 and 70 mm thickness, respectively. Increasing the steel fibers in the concrete mix improved the tensile strength of concrete, resulting in the appearance of the first crack at higher load level and in delaying the stiffness reduction to a higher level of loading. Also, after reaching the cracking load, the stiffness of post cracked zone depended on the amount of steel fibers added to the concrete mix. The higher amount of fibers resulted in a higher stiffness.

Modes of failure

For a two way slab simply supported on all four sides and subjected to a uniform load, failures are generally due to a combination of the two failure modes with the least ultimate load governing the failure of the slab. Usually, bending failure cracks are the first to develop underneath the slabs as applied loading gradually increases and the concrete tensile strength is exceeded. This is because concrete is weak in tension. Typical crack patterns observed underneath the slabs are illustrated in Fig. 8. Collapse may therefore occur either through flexural failure, resulting from the crashing of concrete and/ or fracture of the tension GFRP bars, or shear. The final failure mode, however, depends on the reinforcement ratio and the amount of steel fibers. It is observed from the tests that the addition of steel fibers also increases the strength of two-way slab for both flexural and shear failure.

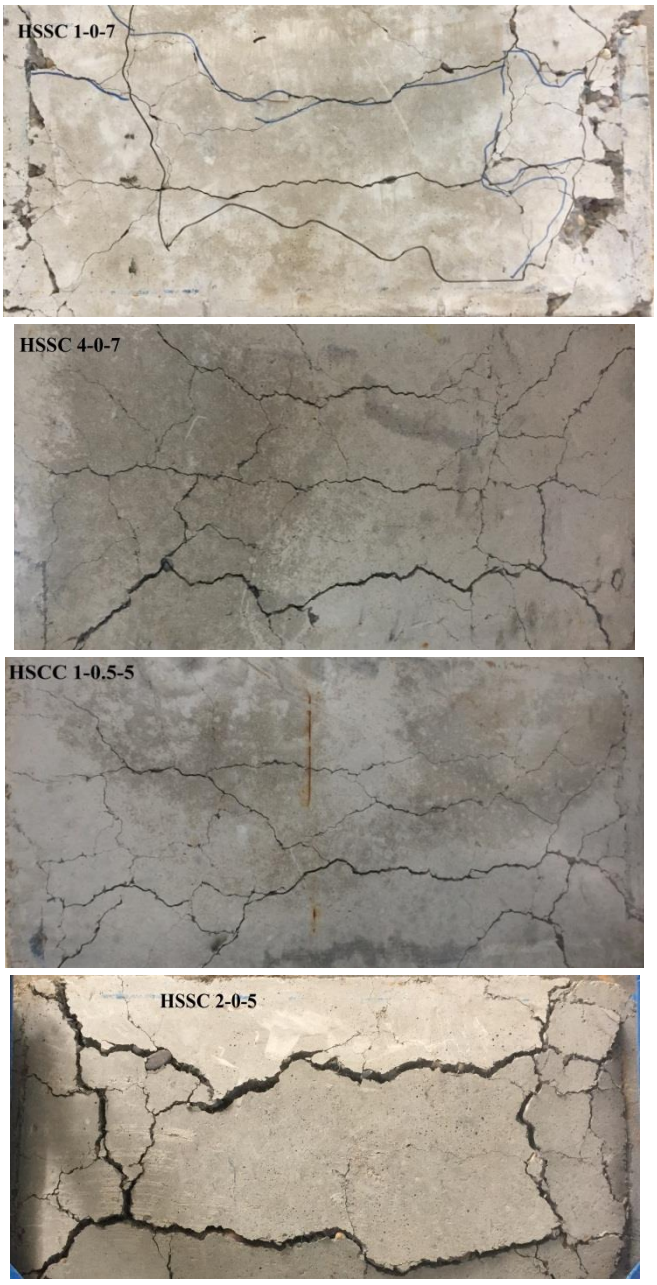

Figure 8. Crack patterns of tested slabs.

THEORETICAL STUDY

To study more thoroughly the structural behaviour of the tested slabs, three dimensional finite element analyses by using ANSYS® (version-R18.2) software is performed. The theoretical study includes, in addition to verifications of all experimental slabs, eight nodes brick element, SOLID-65, with three translations of DOF at each node used to model the FHSC. For FEM modelling of the GFRP reinforcement, two nodes, discrete axial element, LINK-180, with three translations DOF at each node is used. In ANSYS software, the real constants such as cross-section area and thickness are needed to represent the geometry of the used elements. The material properties needed to represent behaviour and

characteristics of constitutive materials depend on mechanical properties such as ultimate strength, modulus of elasticity, Poisson`s ratio and stress-strain relationship. The rectangular mesh is recommended to secure good results from the concrete element (Solid-65), therefore, a rectangular meshing is applied to model all beam specimens.

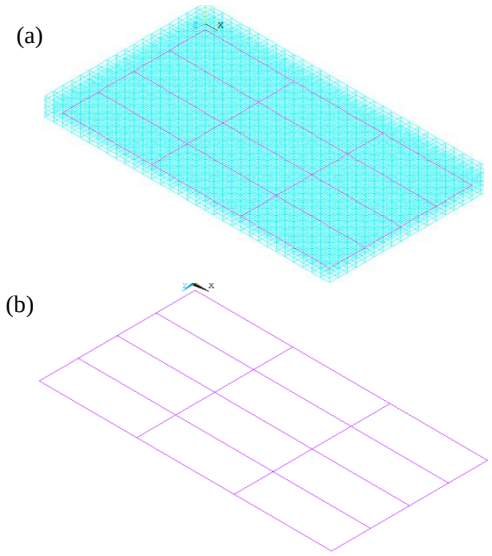

Figure 9. Modelling of reinforcing GFRP bars for slabs: a) GFRP bars positions; b) Link-180 element used for modelling bars.

Load-deflection plots

Deflections (vertical displacements) are measured at mid-span at the centre of the bottom face of beams, in *y*-direction (U_y). Deflected shape of finite element reference slab due to the vertical load is shown in Fig. 10.

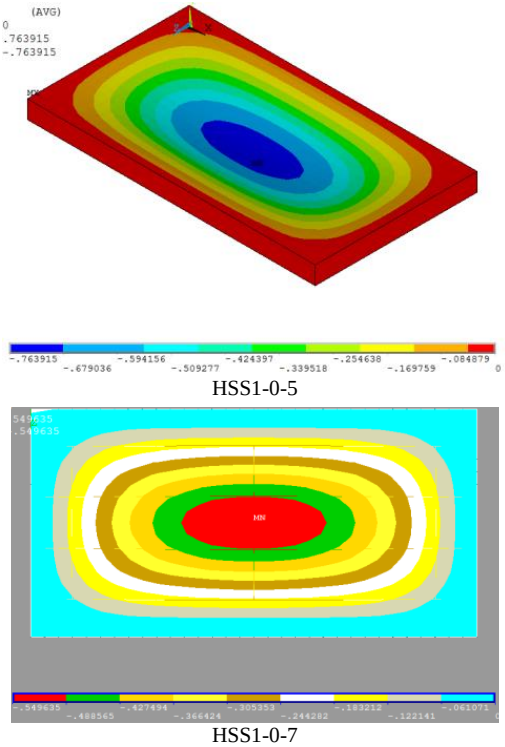

Figure 10. Deflected shape of a tested slab.

The load versus deflection plots obtained from the numerical study together with the experimental plots are presented and compared in Fig. 11. In general, it can be noted from the load-deflection plots that the finite element analyses agree well with the experimental results throughout the entire range of behaviour.

When comparing with experimental values, all numerical models show small deflection at the ultimate stage.

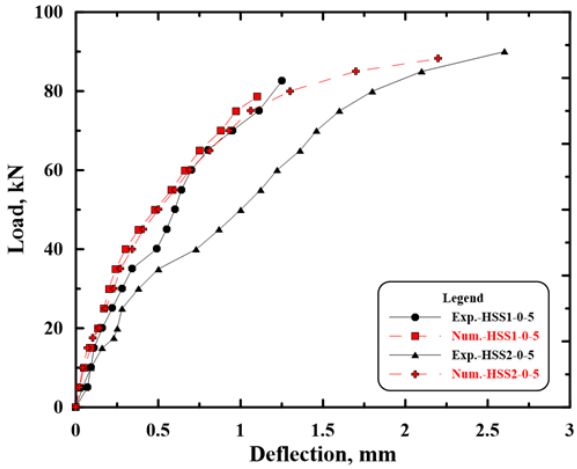

(a) ρ = 0.0048 and ρ = 0.0074, 5 cm slab thickness, V_f = 0

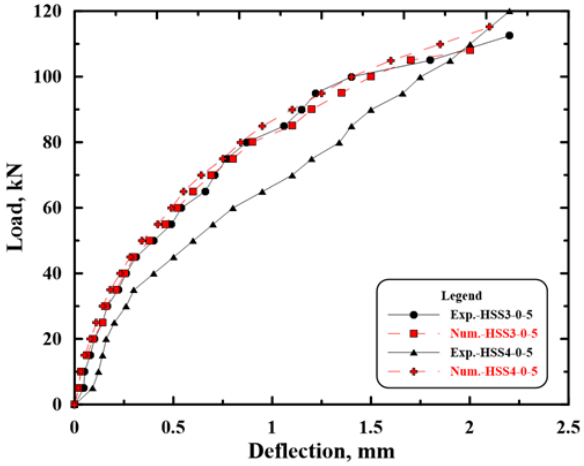

(b) ρ = 0.0096 and ρ = 0.012, 5 cm slab thickness, V_f = 0

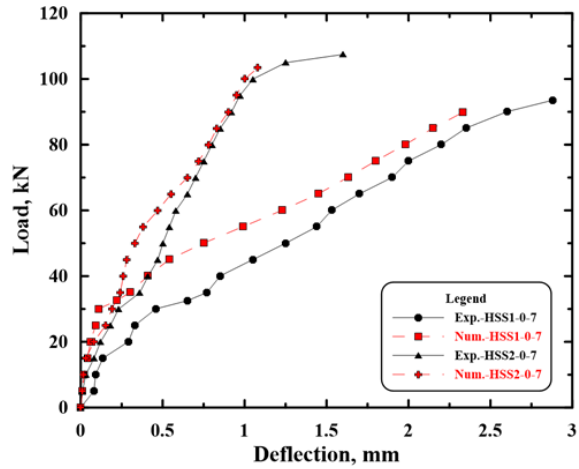

(c) ρ = 0.0032 and ρ = 0.0049, 7 cm slab thickness, V_f = 0

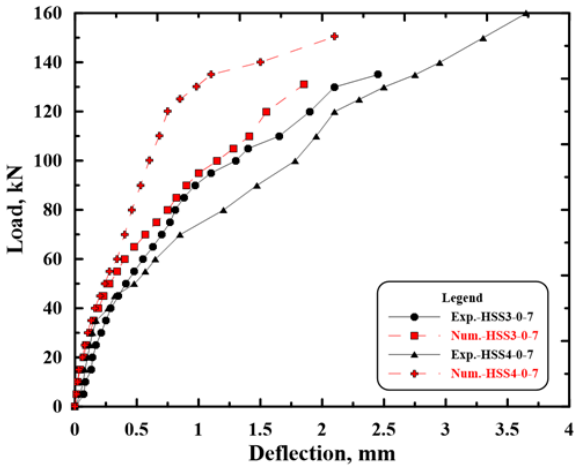

(d) ρ = 0.0064 and ρ = 0.008, 7 cm slab thickness, V_f = 0

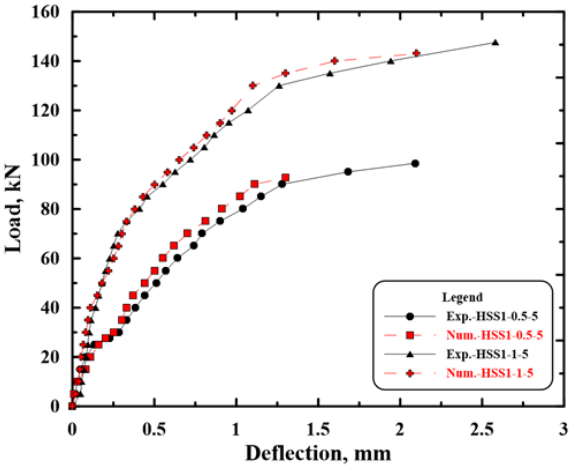

(e) ρ = 0.0048 and ρ = 0.0074, 7 cm slab thickness, V_f = 0.5 and 1

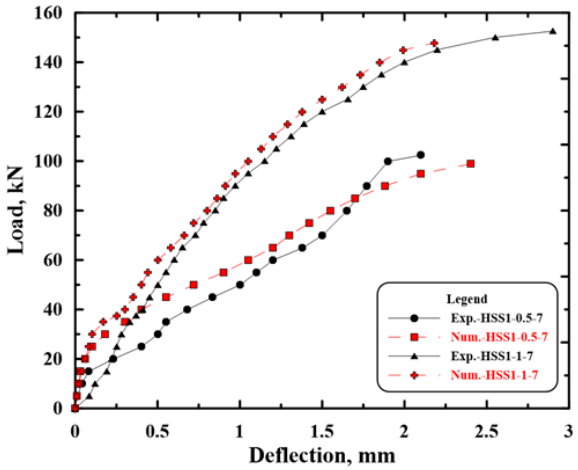

(f) ρ = 0.0032 and ρ = 0.0049, 7 cm slab thickness, V_f = 0.5 and 1

Figure 11. Load-deflection relationship comparison between numerical and experimental.

Ultimate loads

Table 9 shows a comparison between the ultimate loads of the experimental (tested) slabs, $(P_u)_{EXP.}$, and the final loads from finite element models, $(P_u)_{NUM}$. The final loads from numerical models are the last applied load steps before the solution starts to diverge due to numerous cracks and large deflections.

Table 9. Experimental and numerical ultimate loads.

Slab design.	P_{uEXP} (kN)	P_{uNUM} (kN)	P_{uEXP}/P_{uNUM}
HSS1-0-5	82.5	78.6	0.953
HSS1-0-7	93.5	89.75	0.96
HSS2-0-5	90	88.2	0.98
HSS2-0-7	107.5	103.4	0.962
HSS3-0-5	112.5	108	0.96
HSS3-0-7	135	131	0.97
HSS4-0-5	120	115.2	0.96
HSS4-0-7	160	150.4	0.94
HSS1-0.5-5	98.5	92.6	0.94
HSS1-0.5-7	102.5	98.9	0.965
HSS1-1-5	147.5	143.1	0.97
HSS1-1-7	152.5	147.9	0.97

As shown in Table 9, the ultimate loads obtained from the numerical model agree well with corresponding values of the experimental (tested) slabs.

Crack pattern

The ANSYS® program records the crack pattern at each applied load step. Crack patterns obtained from the finite element analysis and the failure modes of the experimental beams agree well, as shown in Fig. 12. The appearance of cracks reflects the failure mode for the slabs. The finite element model accurately predicts failure of slabs in flexure.

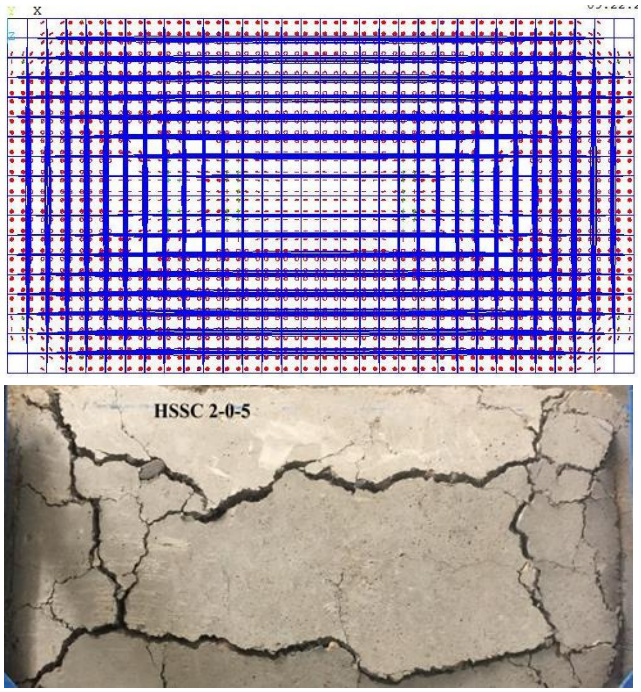

Figure 12. Crack patterns of slabs: from finite element model (above); from experimentally tested slabs (below).

REFERENCES

1. Pendhari, S.S., Kant, T., Desai, Y.M. (2008), *Application of polymer composites in civil construction: A general review*, Comp. Struct. 84: 114-124. doi: 10.1016/j.compstruct.2007.06.007
2. Japan Soc. of Civil Eng. (JSCE), Recommendation for Design and Construction of Concrete Structures Using Continuous Fiber Reinforcing Materials, ed. A. Machida, Concrete Eng. Series No.23, 1997, 325 p.

3. Canadian Stand. Assoc. (CAN/CSA S806-02), Design and Construction of Building Components with Fibre Reinforced Polymers. CSA, Rexdale, Ontario, Canada, 2002, 177 p.
4. American Concrete Institute (ACI 440.1R-06), Guide for the Design and Construction of Structural Concrete Reinforced with FRP Bars, ACI, Farmington Hills, MI, 2006, 44 p.
5. American Assoc. of State Highway and Transport. Officials (AASHTO), AASHTO LRFD Bridge Design Guide Specifications for GFRP-Reinforced Concrete Decks and Traffic Railings, 1st Edition, Washington, D.C., 2009, 68 p.
6. Rizkalla, S., Hassan, T., Hassan, N. (2003), *Design recommendations for the use of FRP for reinforcement and strengthening of concrete structures*, Progress in Struct. Eng. Mater. 5(1): 16-28. doi: 10.1002/pse.139
7. Benmokrane, B., El-Salakawy, E.F., El-Ragaby, A., El-Gamal, S.E. (2007), *Performance evaluation of innovative concrete bridge deck slabs reinforced with fibre-reinforced-polymer bars*, Can. J Civil Eng. 34(3): 298-310. doi: 10.1139/L06-173
8. Demers, M., Neale, K.W. (1999), *Confinement of reinforced concrete columns with fibre-reinforced composite sheets - An experimental study*, Can. J Civil Eng. 26(2): 226-241. doi: 10.1139/cjce-26-2-226
9. Teng, J.G., Huang, Y.L., Lam, L., Ye, L.P. (2007), *Theoretical model for fiber-reinforced polymer-confined concrete*, J Compos. Constr. 11(2): 201-210. doi: 10.1061/(ASCE)1090-0268(2007)11:2(201)
10. Stang, H, Aarre, T. (1992), *Evaluation of crack width in FRC with conventional reinforcement*, Cement Concrete Comp. 14(2): 143-154. doi: 10.1016/0958-9465(92)90007-I
11. Barros, J.A.O., Figueiras, J. (1999), *Flexural behavior of SFRC: Testing and modeling*, J Mater Civil Eng. 11(4):331-339. doi: 10.1061/(ASCE)0899-1561(1999)11:4(331)
12. Vandewalle, L. (2000), *Cracking behaviour of concrete beams reinforced with a combination of ordinary reinforcement and steel fibers*, Mater. Struct. 33(227): 164-170. doi: 10.1007/BF02479410
13. RILEM TC 162-TDF: *Test and design methods for steel fibre reinforced concrete: bending test*, Mater. Struct. (2002), 35 (253): 579-582. doi: 10.1617/13884
14. RILEM TC 162-TDF: *Test and design methods for steel fibre reinforced concrete. Uni-axial tension test for steel fibre reinforced concrete*, Mater. Struct. (2001), 34(235): 3-6.
15. Sorelli, L.G., Meda, A., Plizzari, G.A. (2006), *Steel fiber concrete slabs on ground: A structural matter*, ACI Struct. J, 103(4): 551-558.
16. Alani, A, Beckett, D, Khosrowshahi, F. (2012), *Mechanical behaviour of a steel fibre reinforced concrete ground slab*, Mag. Concrete Res. 64(7): 593-604. doi: 10.1680/macr.11.00077
17. Døssland, Å.L., *Fibre reinforcement in load carrying concrete structures.* Ph.D. thesis; Norwegian Univer. of Science and Technol., Dep. of Struct. Eng., Trondheim, 2008.
18. Pujadas, P., Blanco, A., De la Fuente, A., Aguado, A. (2012), *Cracking behavior of FRC slabs with traditional reinforcement*, Mater. Struct. 45(5): 707-725. doi: 10.1617/s11527-011-9791-0
19. Michels, J., Waldmann, D., Maas, S., Zürbes, A. (2012), *Steel fibers as only reinforcement for flat slab construction - Experimental investigation and design*, Constr. Build. Mater. 26(1): 145-155. doi: 10.1016/j.conbuildmat.2011.06.004
20. Nguyen-Minh, L., Rovňák, M., Tran-Ngoc, T., Le-Phuoc, T. (2012), *Punching shear resistance of post-tensioned steel fiber reinforced concrete flat plates*, Eng. Struct. 45: 324-337. doi: 10.1016/j.engstruct.2012.06.027
21. Wood, R.H., Plastic and Elastic Design of Slabs and Plates: with Particular Reference to Reinforced Concrete Floor Slabs, Thames and Hudson, London, 1961, 344 p.
22. Johansen, K.W., Yield-Line Theory, Cement and Concrete Association, London, 1962, 181 p.
23. Hayes, B. (1968), *Allowing for membrane action in the plastic analysis of rectangular reinforced concrete slabs*, Mag. Concrete Res. 20(65): 205-212. doi: 10.1680/macr.1968.20.65.205
24. Sawczuk, A., Winnicki, L. (1965), *Plastic behavior of simply supported reinforced concrete plates at moderately large deflections*, Int. J Solids Struct. 1(1): 97-110. doi: 10.1016/0020-7683(65)90019-3
25. Park, R. (1964), *Tensile membrane behavior of uniformly loaded rectangular reinforced concrete slabs with fully restrained edges*, Mag. Concrete Res. 16(46): 39-44. doi: 10.1680/macr.1964.16.46.39
26. Al-Shadidi, R.M.H., *Analysis of reinforced concrete square slabs subjected to combined load using yield-line theory*, M.Sc. Thesis, Baghdad University, April 1985.
27. Hassan, A.F., *Effect of membrane action in reinforced concrete slabs*, M.Sc. Thesis, University of Baghdad, Oct. 1982, 175 p.